Seismic safety retrofit of Pitt River bridges

M.Uthayakumar and E.Naesgaard
Macleod Geotechnical Ltd., North Vancouver, B.C.

Abstract: The twin Pitt River bridges located on Lougheed Highway are being considered for seismic upgrading by the Ministry of Transportation and Highways of British Columbia. This paper presents the Geotechnical design and analyses carried out for the upgrading. Assessment of potential sub-soil liquefaction was carried out using the conventional SPT procedures and using a 2-D dynamic analysis, incorporating a liquefaction triggering model. The conventional procedures and the dynamic analyses show that sub-soil liquefaction near the bridges is somewhat limited and sporadic. Displacements of the abutment fill and approach embankments to the bridges were calculated using pseudo-static and 2-D dynamic analyses. Stability of the embankments was assessed using 2-D and 3-D limit equilibrium analyses.

Introduction

This paper describes geotechnical design and analyses carried out for the seismic retrofit of the twin Pitt River bridges. The bridges are owned and operated by the B.C. Ministry of Transportation and Highways (MoTH). Fig. 1 shows the location of the two bridges.

Fig.1. Location of the Pitt River bridges

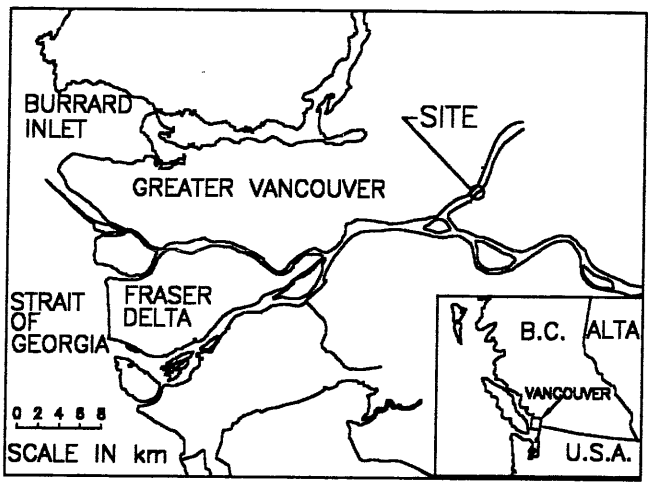

A brief description of the bridges, followed by assessment of slope stability and ground response are given. Ground response analyses were carried out using the computer programs SHAKE (Idriss and Sun, 1992) and FLAC (ITASCA, 1996). FLAC model used for the analyses included liquefaction triggering and post-liquefaction response of the sub-soils. A ground improvement scheme using timber compaction piles and drains is recommended as possible remediation to curtail earthquake induced deformation of sub-soils.

Description of the bridges

The bridges are located on Lougheed Highway, across the Pitt River, between Port Coquitlam and Pitt Meadows, British Columbia. The older, downstream bridge carries two-lanes of east bound traffic, and the upstream bridge carries two-lanes of west bound traffic. The upstream bridge is approximately 76m north of the downstream bridge.

The downstream bridge was constructed in the early 1910s and major renovations were carried out in 1955. The bridge is about 334 m long between the two abutments, and consists of eight fixed spans and a central swing span. Fig. 2 presents the plan and a generalised sub-soil profile under the bridge.

The abutments were replaced in 1955 and are founded on vertical and battered steel H piles. The west abutment is supported by two pile groups. Each group consists of 6 piles, the 3 piles on the river side are battered at 3V:1H, and the 3 piles on the back are vertical. The east abutment is also supported by two pile groups. Each group consists of 9 piles, the 3 on the river side are battered at 4V:1H, the middle 3 battered at 8V:1H and the 3 piles in the back row are vertical. Pier 1 (numbered starting from the west side, as shown in Fig. 2), which was also added in 1955, is supported by 20 vertical steel H piles. Pier number 9, which was originally supported by timber piles, was rehabilitated in 1955 by adding 10 steel H piles around the timber piled foundation. The remaining piers, from 2 to 8, are founded on timber cribs. The timber cribs are approximately 6 m by 11m in plan, jetted to a depth of approximately 10.7m below ground level. The cribs had a steel cutting edge around the bottom perimeter and across the centre, and were covered with 50mm timber sheeting on the outside. Following jetting down to the design level, the inside of the cribbing was partially filled with concrete

The upstream bridge was built in the late 1970s, northeast of the downstream bridge. The bridge is approximately 361 m long between the two abutments, and is supported by 9 piers (see Fig. 3). The piers are founded on 610mm diameter concrete filled steel pipe piles. Each pier is supported by 16 to 25 piles of 50 to 60 m length. The abutments are supported by raft foundations, bearing on compacted sand and gravel fill.

A control tower, located in between the two bridges, was also built in the late 1970s, supported by 610mm concrete filled steel pipe piles. Bridge traffic is monitored by remote TV cameras and the swing spans of both the downstream and the upstream bridges are operated from the control tower. Boats in the river are allowed to navigate through the bridges

Fig. 2. Plan and generalized sub-soil profile of the downstream bridge

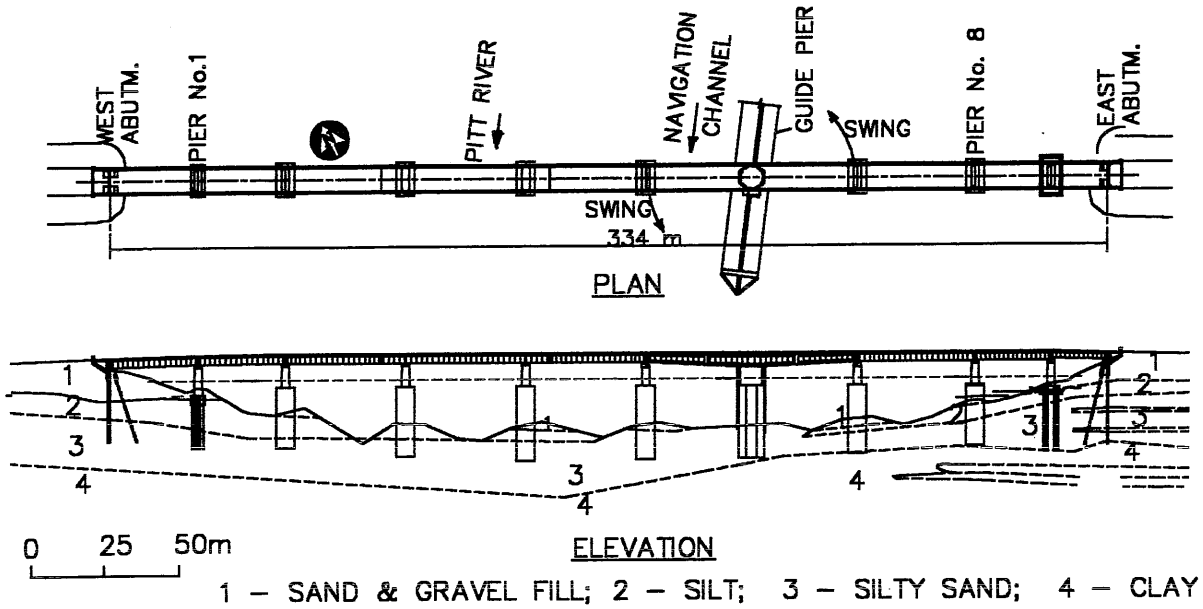

Fig. 3. Plan and generalized sub-soil profile of the upstream bridge

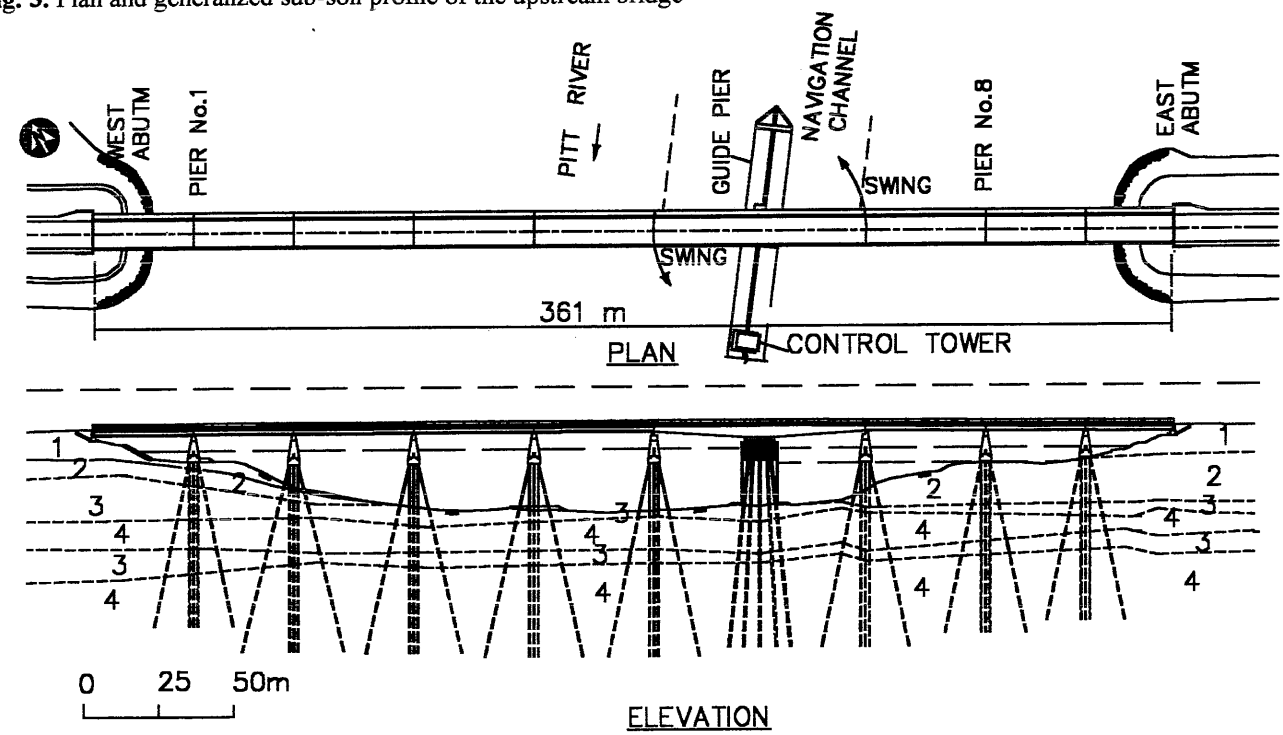

by opening the two swing spans. Guide piers together with Pier No. 6 of each bridge support the swing spans when they are opened for river traffic (Figs. 2 and 3).

Site investigation and soil profile

Soil data from the test holes drilled in 1912, 1972, 1974 and 1976 for the construction of the bridges were augmented by test holes drilled in 1996 and 1999. The test holes and the investigations were carried out by the MoTH. Rotary test holes with Standard Penetration Tests (SPT) and Shelby tube sampling were included in the 1972, 1974, 1976 and 1999 investigations. Laboratory tests, including grain size analyses, moisture contents, Atterberg limits, consolidation tests, vane shear tests, unconfined compression tests and consolidated undrained triaxial tests were carried out on selected soil samples. Static and seismic cone penetration tests (CPT and SCPT) were carried out with the 1996 and 1999 investigations.

Two pile load tests were carried out in 1973 as part of the design of the upstream bridge. 610 mm diameter steel pipes

with a wall thickness of 12.5mm were used for test as well as production piles. The piles were driven with open end near the existing east abutment of the upstream bridge to depths of 35 m and 55 m. After driving to the required depth, the inside of the pipes were cleaned out and filled with concrete. Ultimate axial capacities of 1511 kN and 3333 kN were achieved from the tests for the 35 m and 55m long piles respectively (Crippen & Associates, 1974).

Test hole data indicate that both east and west approach embankments were constructed of sand and gravel fill. At the abutments the fill is approximately 10 m thick. A layer of low plastic silt with thin sandy inter-layers exists below the sand and gravel fill. The thickness of this silt layer appears to increase towards the east abutment of the upstream bridge. Some rip-rap gravel fill (0 to 5 m thick), placed as scour protection, exists around the jetted-in piers of the downstream bridge. A loose sand layer overlies low to high plastic clay layer. Bottom of the jetted-in piers 2 to 6 rest within the loose sandy layer and the bottom of piers 7 and 8 rest within the clay layer. The pipe piles of the upstream bridge were also driven into the clay layer to depths of 50 to 60 m. Figs. 2 and 3 show the interpreted soil profile in detail.

A seismic reflection survey indicates that the "firm ground" (very dense Pleistocene soils) or bedrock depth is about 115 m below the western edge of the river (MoTH, 1999). For the analyses the depth to the "firm ground" or bedrock is assumed to be the same (115 m) throughout the site.

Seismicity

The Pitt River Bridges have been classified as "Lifeline Bridges" by MoTH (1998). A "Lifeline Bridge" should not collapse due to the design earthquake, but may suffer repairable damage.

The design earthquake motion selected by MoTH has a 10% probability of exceedance in 50 years (equivalent to a return period of 475 years) and a Peak Ground Acceleration (PGA) of approximately 0.24g. The "firm ground" design response spectrum is shown in Fig. 4. It is a site specific Uniform Hazard Response Spectrum (UHRS) obtained for 5% damping.

Three sets of orthogonal "firm ground" acceleration-time histories for use in the design were fitted to the design spectrum by Dr. Anderson of Cherry, Anderson and Nathan (CAN). The acceleration spectrum of each modified record closely matches the "firm ground" design spectrum shown in Fig. 4. Only horizontal ground motions were considered for geotechnical design.

Ground response analyses

Several ground response analyses were carried out for selected locations across the river using the 1-D computer program SHAKE91 (Idriss and Sun, 1992). The objectives of the ground response analyses are to:

- develop site-specific, near-surface design spectra for structural analyses,
- provide time histories and calibrate soil shear moduli for the 2-D dynamic analyses (using the program FLAC), and
- estimate cyclic stress ratio for liquefaction assessment.

Fig. 4. Design acceleration spectra with 5% damping for "firm ground" and near-surface

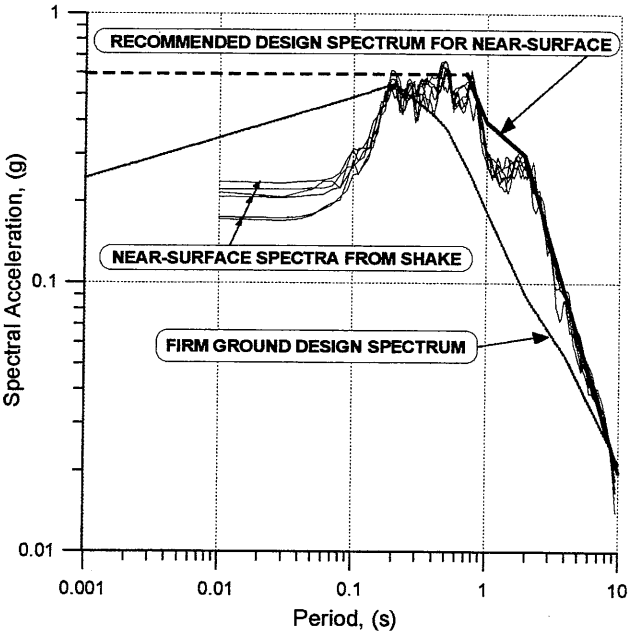

Shear wave velocity profiles obtained from the SCPT holes were used as soil input parameters in the analyses. Shear modulus reduction and damping curves used were obtained from published data on similar soils (Seed and Idriss, 1970, Sun et al, 1988 and Vucetic and Dobry, 1991).

Near-surface acceleration response spectra obtained from the ground response analyses are presented in Fig. 4 together with the "firm ground" design spectrum. PGA and Cyclic Stress Ratio (CSR) profiles obtained from SHAKE are shown in Fig. 5a and 5b respectively. CSR is defined as $0.65\tau_{max}/\sigma'_v$, where τ_{max} is the maximum shear stress and σ'_v is the vertical effective over-burden stress within each soil layer considered in the SHAKE analyses. The PGA and CSR profiles shown in Fig. 5 were obtained using soil profiles representative of the middle of the upstream bridge for one of the design input motions. Similar profiles were obtained for the other five design input motions. From all six CSR profiles at a given location, an average profile was developed. Also, several CSR profiles were developed across the length of each bridge for liquefaction assessment.

The input time history for the 2-D dynamic FLAC analysis was obtained from SHAKE at the elevation of the base of the FLAC grid. A baseline correction was carried out to the motion obtained from SHAKE so that all acceleration, velocity and displacements are zero at the end of shaking.

In the 1-D SHAKE analyses shear stresses induced by the abutment embankments on the sub-soils were not considered. The ground surface was taken as the top of each test hole with infinite lateral extent. The response of the sub-soils under the abutment embankments, with initial static shear stresses was assessed separately using the 2-D dynamic FLAC analyses.

Fig. 5. (a). Peak ground acceleration and **(b).** cyclic stress ratio profiles from SHAKE analyses

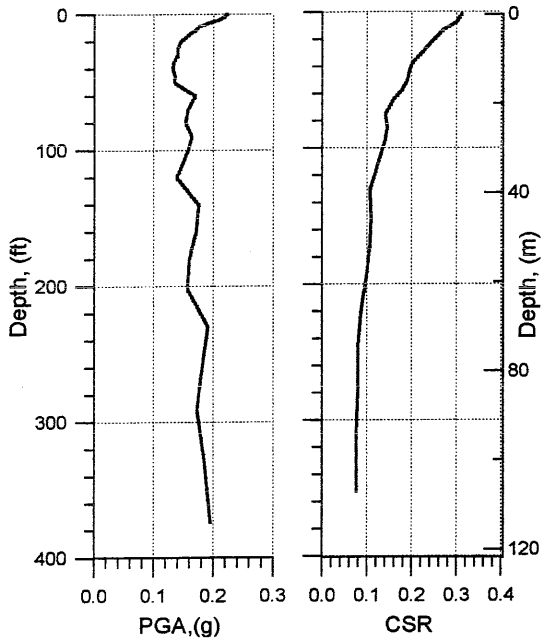

Slope stability analysis

Stability of the approach embankments and abutment fill slopes were first assessed using 2-D slope stability program XSTABL (Interactive software designs, 1996). The analyses indicate that under static loading the approach embankment and abutment fills are only marginally stable, whereas the riverbank slopes away from the abutment fill show larger factor of safety against sliding. Table 1 shows the soil properties used in the analyses.

Table 1. Soil properties used in the slope stability analyses

Soil type	Unit weight (kN/m^3)	Friction angle (deg.)	Cohesion (kPa)
1. Sand & gravel	20.0	40	-
2. Silt	17.5	-	25 – 40
3. Silty sand	18.5	32	-
4. Clay	17.5	-	50 – 100

To account for the limited lateral extent of the approach embankment and abutment fill slopes, two different types of 2-D analyses were carried out;

- Shallow failure surfaces – Stress increment due to the embankment will be highest at shallow depths, below the embankment. To assess the stability of slopes with shallow failure surfaces, the full height of the embankment was used. The failure surfaces were forced to be shallow as shown in Fig 6.
- Deep-seated failure surfaces – Stress increase due to the embankment will decrease with depth (due to the limited lateral width of the embankment). The stresses calculated with the full height of embankment and 2-D plane strain assumption will not be valid for deeper layers. Therefore, an equivalent or reduced height of embankment to represent 2-D plane strain state was obtained. The equivalent height of the fill was estimated assuming that the fill of both abutments is spread between the two extreme ends with a constant thickness.

Fig. 6. 2-D slope stability analysis of the east abutment fill – shallow failure surfaces

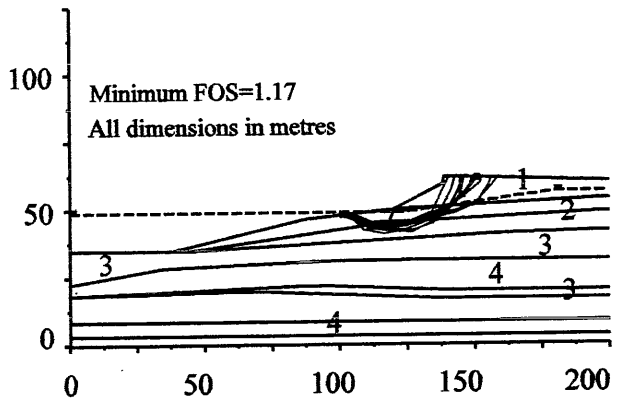

2-D slope stability analyses were carried out using the computer programs XSTABL (Interactive software designs, 1996) and CLARA (Hungr, 1988). Possible shallow and deep-seated failure surfaces were analysed separately. The analyses indicate factors of safety of 1.2 and 1.3 for shallow and deep-seated failure surfaces respectively for the downstream bridge east abutment fill (see Figs. 6 and 7). These factors of safety are for static loading with the lowest water level in the river. Increasing the water level in the river to that of mean level did not increase the factor of safety significantly. Note that the elevation difference between the lowest and mean river levels are approximately 2 m, which is small compared to the scale of the slopes analysed.

Following the 2-D analyses, 3-D slope stability analyses were carried out in order to assess the effect of the approach embankments in detail. The limit equilibrium slope stability program CLARA (Hungr, 1988) was used. For shallow failure surfaces the factors of safety calculated from the 2-D analyses agreed reasonably with the 3-D analyses. On the other hand, factors of safety for deep-seated failure surfaces in 3-D analyses agree with those of 2-D analyses for

riverbank slopes (with no approach embankment or abutment fill). Table 2 presents factors of safety obtained from the 3-D analyses for shallow failure surfaces. Fig. 8 shows a typical shallow failure surface obtained from CLARA.

Table 2. Factors of safety for static loading from 3-D analyses

Slope analysed	Factor of safety
Downstream bridge east side	1.3
Downstream bridge west side	1.6
Upstream bridge east side	1.4

Fig. 7. 2-D slope stability analysis of the east abutment fill – deep-seated failure surfaces

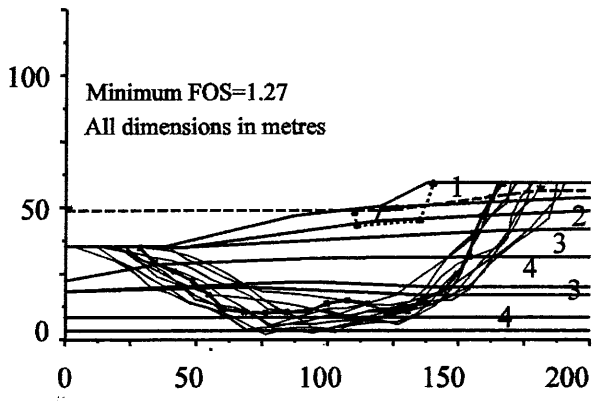

Fig. 8. Sliding surface of the downstream bridge east abutment fill – 3-D analysis

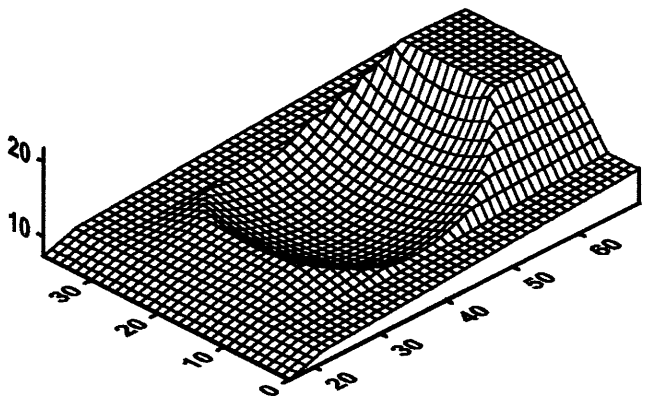

Seismically induced displacement of the abutment fill

Seismically induced displacements of the abutment fill slopes were assessed using the 2-D limit equilibrium slope stability analyses and Newmark (1965) procedure. Yield accelerations (the acceleration which gives a factor of safety of 1.0 for seismic loading) of the slopes were obtained from the slope stability analyses. Seismically induced displacements were calculated by numerical integration of the excess acceleration history over the yield acceleration. Integration was carried out for those time intervals when the excess acceleration is positive and for sufficient time when the difference is negative so that the final velocity is zero for each occurrence of positive excess acceleration (Castro, 1987).

Fig. 9 shows a displacement time history typical of the results. Table 3 summarises the calculated yield accelerations and displacements of each of the abutments. Note that the displacements calculated do not include those induced by possible liquefaction of loose sandy soils. Sub-soil liquefaction and its effects are described in the following sections. The acceleration time histories used in the calculations are those taken at a depth of 1 m below grade from SHAKE analyses. For the seismic analyses, water level in the river was assumed to be the mean river level, as it was deemed unlikely that the design earthquake and the lowest water would occur simultaneously.

Table 3. Seismically induced displacements of the abutments

Abutment location	Yield acceleration (g)	Displacement (mm)
Downstream east	0.050	290
Upstream east	0.035	550
Downstream west	0.060	180
Upstream west	0.075	90
River bank slope	0.085	55

Fig. 9. Seismically induced displacement of the downstream bridge east abutment fill – Newmark (1965) analysis

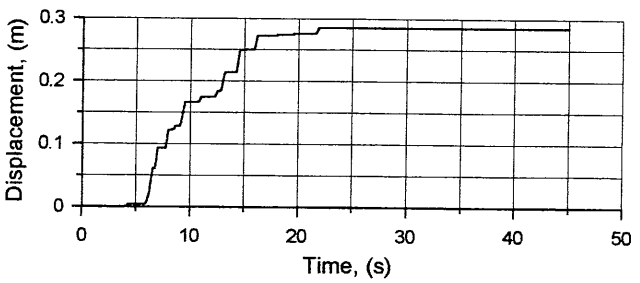

Liquefaction assessment

Liquefaction assessment of the sub-soils was carried out using the following two procedures;

- Conventional Seed and Idriss (1982) method with cyclic stress ratio (CSR) obtained from the SHAKE analyses and
- 2-D dynamic analyses using the program FLAC with liquefaction triggering.

For the Seed and Idriss (1982) method cyclic resistance ratio (CRR) of the sub-soils, earthquake magnitude weighting factor K_m and overburden stress correction factor K_σ were obtained using the procedures recommended by (Youd and Idriss, 1997). The induced CSR by the design ground motions were obtained from SHAKE analyses as discussed previously. Factor of safety against liquefaction was estimated as the ratio of CRR/CSR.

The above analyses indicate that the extent of sub-soil liquefaction is somewhat limited and sporadic for the assumed design earthquake. Fig. 10 presents the liquefaction assessment results where some liquefaction potential was noted (SCPT2/96 and BH1/99, drilled near the down stream bridge east abutment).

Fig. 10. Typical cone penetration test data and factor of safety (F.S.) against liquefaction – Downstream bridge east abutment

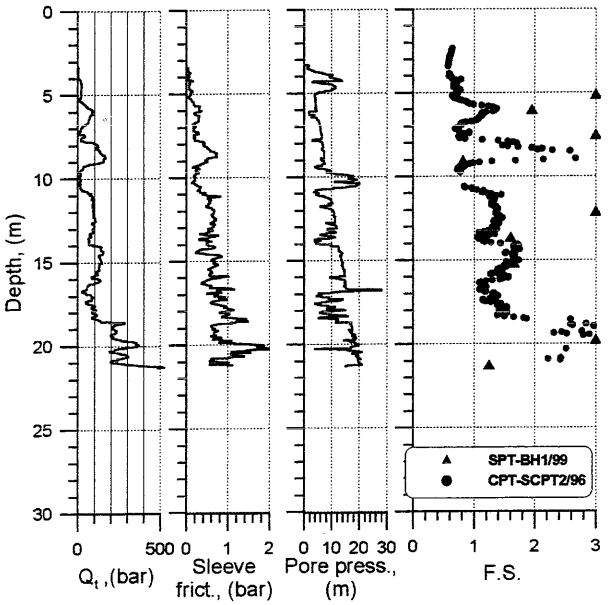

Dynamic analysis with liquefaction triggering

Liquefaction triggering and resulting ground deformations were assessed using a 2-D dynamic FLAC (ITASCA,1996) analysis. A liquefaction triggering model, developed at UBC (Beaty & Byrne, 1999) was incorporated in the analysis. The response of the soil, including those of pre-liquefaction, liquefaction triggering and post-liquefaction were captured in this method of analysis.

The analysis was carried out by first solving the problem for static loading conditions. With the stress state at static conditions, dynamic loading (earthquake shaking) was started with an input motion at the base of the grid. For the dynamic loading, lateral boundaries of the grid were set to "free field boundaries" (Itasca, 1996)

In the liquefaction triggering model, cyclic stress ratio (CSR) induced within each element of the grid are calculated and compared to the cyclic resistance ratio (CRR). CRR is obtained from $(N_1)_{60}$ values using Seed's chart (Seed and Idriss, 1982), with corrections for over-burden stress level, K_σ. No correction for the earthquake magnitude is performed, as the correction is accounted for in the specified design earthquake motion used. The number of "equivalent cycles of loading" within each element during dynamic loading is monitored. Liquefaction is assessed based on the relationship between the number of cycles and CSR to cause liquefaction (Beaty and Byrne. 1999). For the current assessment a factor of safety of 1.0 was used together with the calculated CSR.

After liquefaction the stress-strain model of the liquefied element is changed to that of a post-liquefaction model. Input parameters for the post-liquefaction model are residual shear strength and limiting shear strain (minimum shear strain at residual strength). Shear modulus for the loading portion of a cycle is calculated as the ratio of residual shear strength to the limiting shear strain, and the unloading modulus is set to ten times that of the loading modulus. Bulk modulus is set to twenty times the loading shear modulus.

Fig. 11 shows the FLAC grid used for the analysis of the downstream bridge sub-soils. Both the full height of the approach fill embankments, and the equivalent or reduced height described earlier, were used in separate analyses. Elevation of the water was taken as the mean river level.

Pre-liquefaction soil properties used are presented in Table 4. For liquefaction triggering $(N_1)_{60}$ obtained from various test holes along the section were used. Based on the $(N_1)_{60}$ values and the relationship proposed by Byrne and Beaty (1999), residual shear strength of the sandy soils were assumed to be 0.24 times the vertical overburden stress (i.e. $S_u/p' = 0.24$). The limiting shear strain was assumed to be 4% (Byrne and Beaty, 1999).

Table 4. Pre-liquefaction soil properties used in the dynamic analyses

Soil layer No.(*)	Density (kg/m^3)	Secant shear modulus (MPa)	Bulk modulus (MPa)	Cohes-ion (kPa)	Frict-ion angle (deg.)
1	2000	10.4	208	0	40
2A	1750	13.1	262	25	0
2B	1750	13.1	262	40	0
3	1850	18.9	378	0	32
4A	1750	29.5	590	50	0
4B	1750	29.5	590	70	0
4C	1750	29.5	590	100	0

(*) - See Fig. 11 for soil layers

Soil damping for the FLAC analyses was obtained using an iterative procedure in which results from SHAKE and a 1-D FLAC analyses were compared. Damping for the 1-D FLAC analysis was varied until the surface acceleration

Fig. 11. FLAC model used in the 2-D dynamic analyses

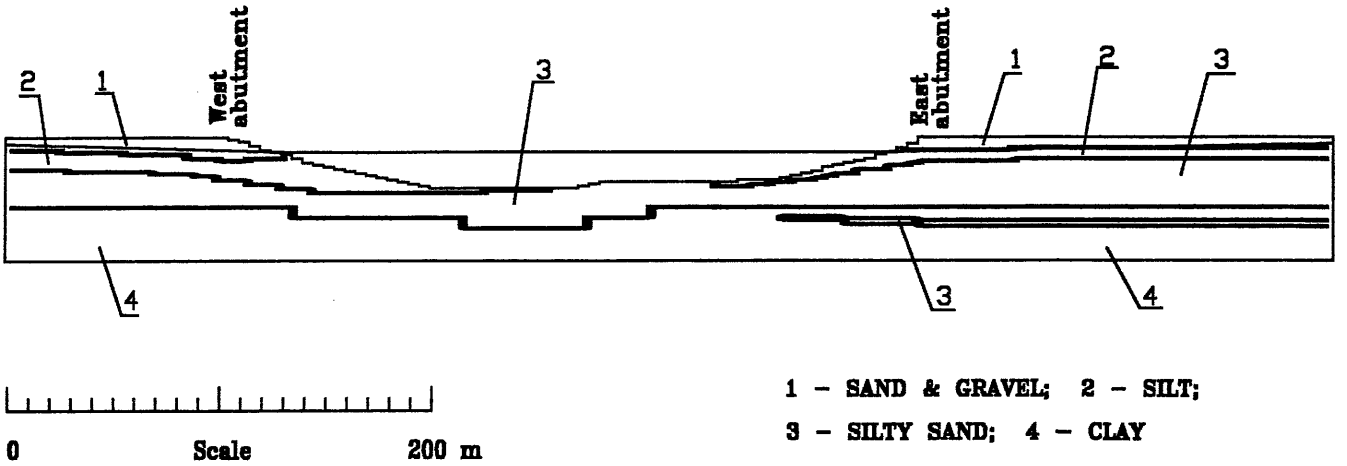

history from FLAC matched that from SHAKE. Based on the above procedure 7% Rayleigh damping with a central frequency of 5 Hz (ITASCA,1996) was chosen for further 2-D FLAC analyses.

Fig. 12 presents the input motion used in the dynamic analyses. Note that the base of the grid where the input motion was applied is not the "firm ground". The motion was obtained from SHAKE analysis using the "firm ground" motion and taking out an acceleration history at the level of the FLAC grid base. The acceleration history was baseline corrected to make velocity and displacement values zero at the end of shaking.

Fig. 12. Input motion used in the FLAC analyses

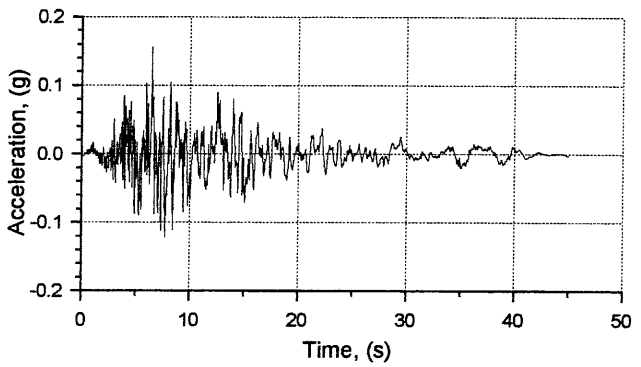

Results of the dynamic analyses

Fig. 13 shows the horizontal displacement contours of a typical analysis with the equivalent or reduced embankment height. Horizontal displacement time histories for selected points at the ground surface are presented in Fig. 14. Locations of the points are shown in Figs. 13 and 14 with numbers from 1 to 6. Positive displacements are from left to right horizontally, and upwards vertically. Extent of sub-soil liquefaction from the dynamic analysis is presented in Fig. 15. Fig. 14 indicates that the permanent movement of the west and east abutments towards the river are approximately 400 mm and 800 mm respectively. Note that the above displacements are the cumulative of those from pre and post-liquefaction states. The Newmark's (1965) procedure, with no sub-soil liquefaction, indicates displacements of the west and east abutments are approximately 180 mm and 290 mm respectively (Table 3).

Similar analysis with the full height of embankment shows horizontal displacement of the west and east abutments are about 500 mm and 2000 mm respectively. Analysis with no abutment fill shows that the riverbank slopes may move approximately 75 mm towards the river due to the design earthquake shaking.

The 2-D analysis with the full embankment height was used to obtain the response and deformation pattern at shallow depth. Analyses with the equivalent or reduced embankment height were carried out to obtain deep-seated deformation patterns.

To limit the deformation of the abutment fill and embankments, various ground improvement methods were reviewed and timber-compaction piles with drains were selected. For the analysis the FLAC grid with the full embankment height was revised to include the timber-compaction piles. The piles were introduced as structural elements (ITASCA, 1996) within the soil model. Pile embedment depth of 20 m and spacing of 1.4 m were used in the analysis. Densification widths of 15 m and 20 m were used near the west and east abutments respectively.

Fig. 16 shows the displacement contours with timber compaction piles. Extent of sub-soil liquefaction following ground densification is shown in Fig. 17. Note that the deformation of the east abutment area has been reduced from approximately 2000 mm to about 300 mm following ground improvement.

Fig. 13. Horizontal displacement contours

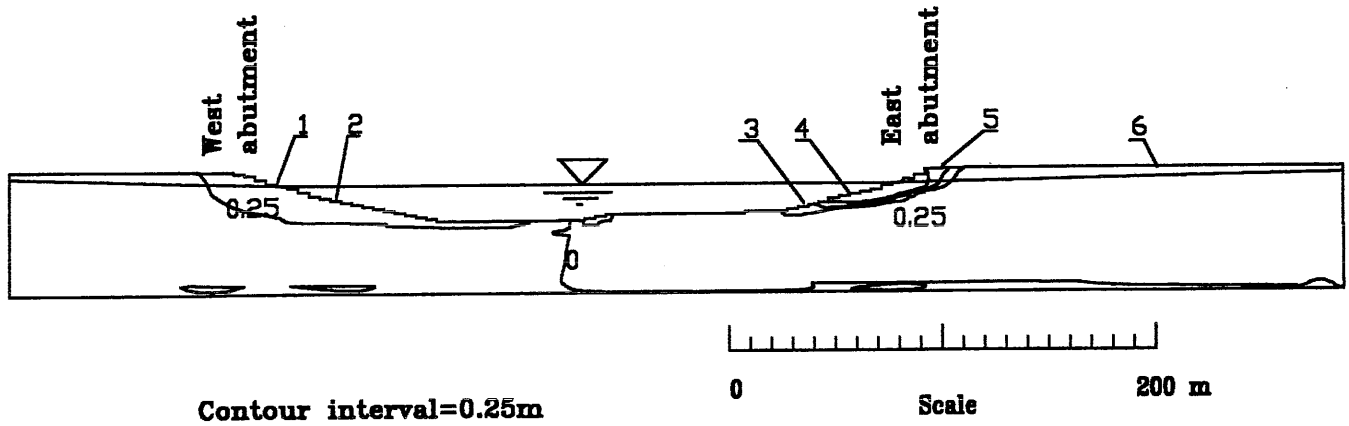

Fig. 14. Horizontal displacement history of selected points on the surface

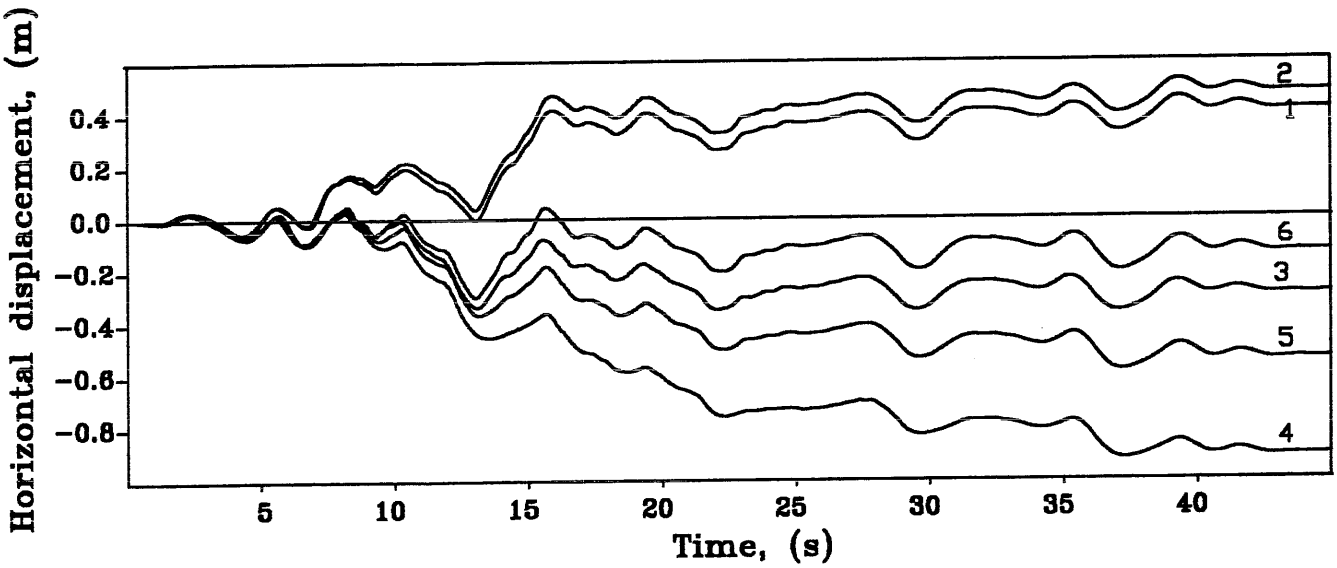

Fig. 15. Extent of sub-soil liquefaction near the downstream bridge – equivalent embankment height with no densification

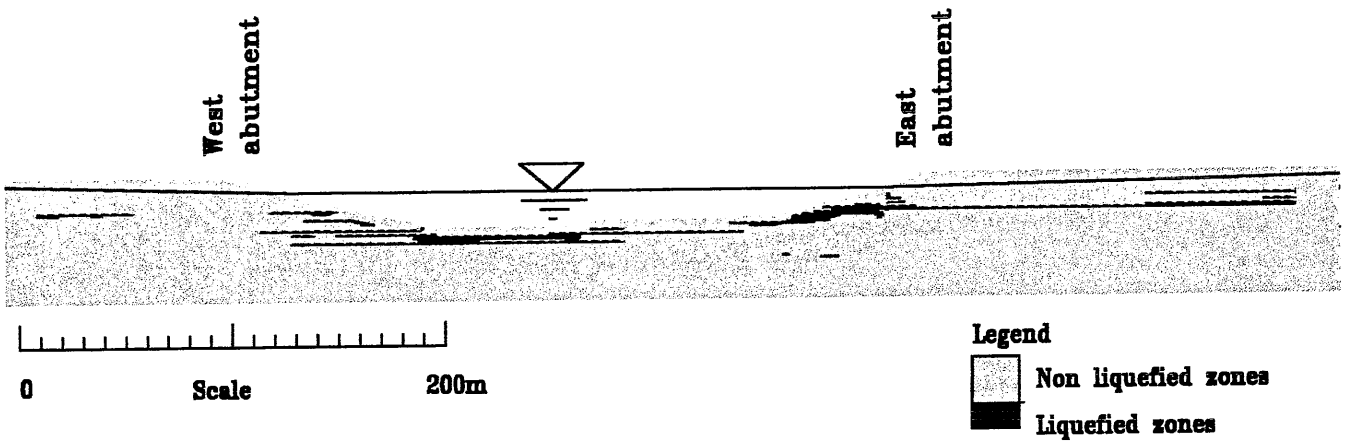

Fig. 16. Displacement contours near the east abutment – after ground improvement with timber compaction piles

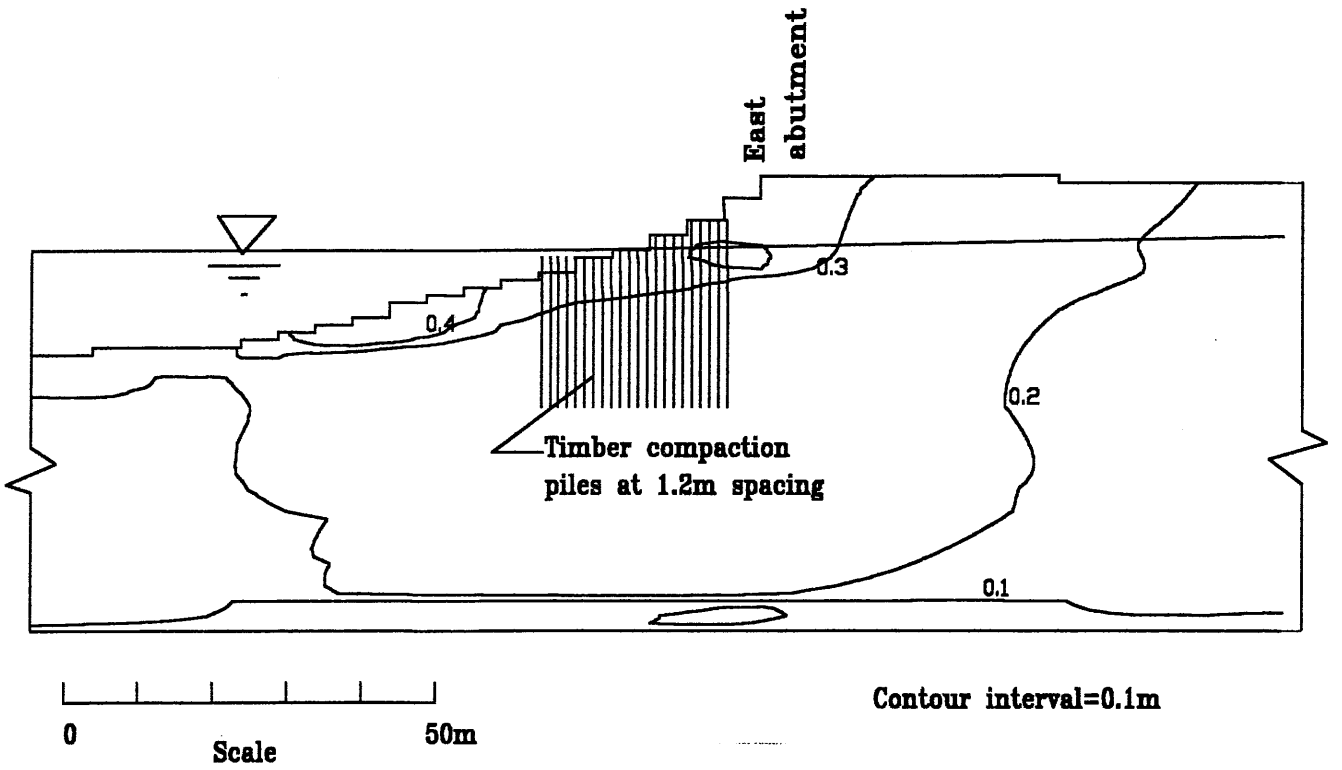

Fig. 17. Extent of sub-soil liquefaction near the downstream bridge – after densification

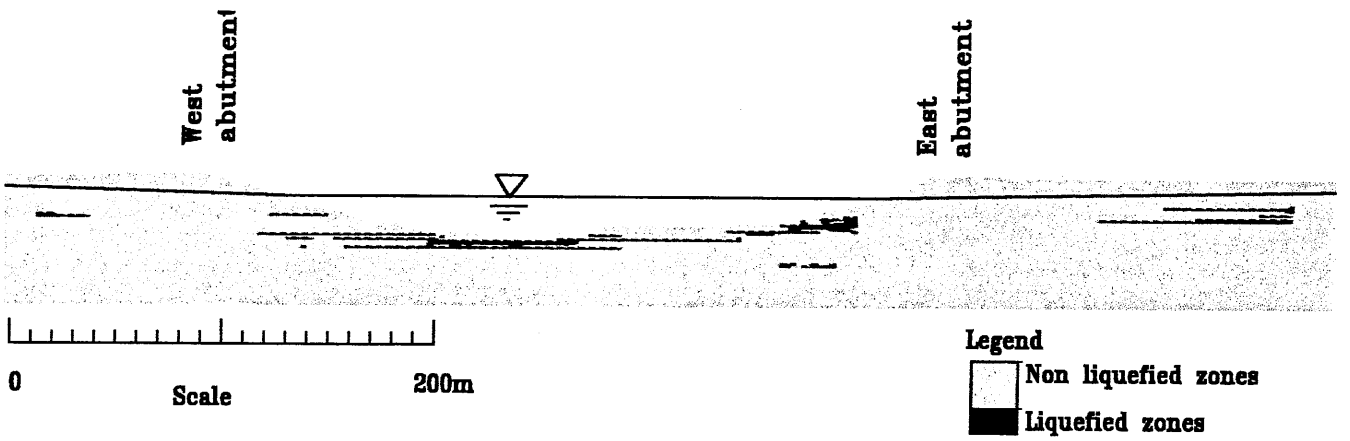

Discussion of the dynamic analyses

The dynamic analyses described above uses a state-of-the-practice method for evaluation of liquefaction and ground deformation. This method of analysis models the response of soil structures more correctly than those which use pseudo-static methods. However, the analysis uses a total stress model for the soils and generation of pore water pressure during dynamic loading is not estimated. The analysis also assumes that the soils remain undrained during earthquake shaking (i.e. no pore water pressure migration between elements). In a natural deposit of soils with varying densities, permeabilities etc., the assumption that the soils remain undrained during earthquake loading may not be exactly true. Pore water may migrate from the loose sandy layers which develop higher pore water pressure into the dense layers. Recent large scale model tests and centrifuge tests indicate shaking of a multi-layered soil deposit may result in formation of thin water layers at the boundaries (Kokusho,

1999, Balakrishnan and Kutter, 1999). These water layers, which have zero shear strength, accumulate at the bottom of relatively impermeable silt or clay layers. The current analyses do not model pore water migration nor the water layers. However, the residual shear strengths used were obtained from back analysis of liquefaction induced failures (Byrne and Beaty, 1999). Note that Byrne and Beaty (1999) developed the residual shear strength ratio - $(N_1)_{60}$ relationship using the data base from Seed and Harder (1990). The back calculated residual strengths, therefore, would have included the effects of pore water migration and possible water layers. It is recognised that there is a large uncertainty in the selection of appropriate residual shear strengths, whether it is from laboratory tests or from past experiences. This uncertainty should be considered in interpreting the results.

In developing a ground improvement plan for densifying the potentially liquefiable layers, consideration should also be given to the formation of water layers in a multi-layered soil deposit. Excess pore water pressure will develop in soils during shaking, irrespective of the density, and whether it liquefies or not. To densify the liquefiable layers and to improve the shear strength of silt layers, timber compaction piles have been considered for this project. In addition, provision of drainage columns is also recommended. It is proposed to install the drainage columns along the centreline of the densification zone.

Other consequences of liquefaction

Lateral spreading of sub-soils around the piles supporting the piers may cause piles to deform and, in some cases, may lead to failure of the piles. Also, earthquake shaking will cause build-up of pore water pressure, and therefore reduce effective normal stresses in all soil layers (both, liquefiable and non-liquefiable). This reduction in effective stresses will cause a temporary reduction in pile capacities. However, the temporary reduction in capacity is not expected to cause bearing failure of piles which are designed with adequate factor of safety for static loading. Post-liquefaction consolidation settlement may also induce down-drag on the piles. Note that the analyses indicate sub-soil liquefaction is somewhat limited, sporadic, and not continuous across the bridge sub-soils.

Lateral loading response of piles due to seismically induced ground deformation was assessed using the program LATPILE (Byrne and Janzen, 1985). Magnitudes and pattern of ground deformation - used as "free field" input for the LATPILE analyses - were derived from the 2-D dynamic FLAC analyses described earlier. Pile deformation, moment and shear within the piles were assessed in the LATPILE analyses and found to be within tolerable limits.

Settlement from consolidation of the liquefied layers was assessed using the procedures of Tokimatsu and Seed (1987). Settlements in the order of 50 mm were estimated under the bridge abutments. This settlement is additional to those obtained from the 2-D dynamic FLAC analyses.

Conclusions

The twin Pitt River Bridges are being considered for seismic upgrading. Geotechnical components of the upgrading work include:

- Assessement of existing soil data from previous investigations and new site investigations, field tests and laboratory tests on soil samples.
- Ground response analyses using design earthquake input motions. The input motions were fitted to a site specific Uniform Hazard Response Spectrum. The design ground motion has a probability of exceedance of 10% in 50 years or has a mean return period of 475 years
- Slope stability analyses of the approach embankments and abutment fill. 2-D and 3-D slope stability analyses indicate possible shallow and deep-seated failure surfaces with factors of safety 1.3 and 1.2 respectively for static loading.
- Assessment of liquefaction potential of sub-soils. Conventional analyses and 2-D dynamic analyses indicate somewhat limited and sporadic liquefaction of sub-soils across the bridge alignment.
- Estimation of seismically induced deformations using pseudo-static analyses and 2-D dynamic analyses. Displacements in the range of 90 to 2000 mm were estimated for the various abutment fill and slopes.
- Potential remediation work. To limit the displacements of abutment fill and embankments, timber compaction piles with drains were considered. Analyses indicate that a 20m wide strip of timber compaction piles driven at 1.2 m spacing could potentially reduce the displacements from 2000 to 300 mm. This reduction in ground deformation is achieved by densifying the ground against liquefaction and by improving the shear strength of the shallow silt layers.

Acknowledgement

Authors wish to thank the B.C. Ministry of Transportation and Highways (MoTH) for giving permission to publish this paper. Buckland & Taylor Ltd. is the prime and structural consultant for this project. Authors would like to thank Dr. Don Gillespie and Mr. William Szto of the MoTH and Dr. Peter Taylor and Dr. Steve Zhu of Buckland & Taylor Ltd. for the opportunity to work on this project. Also, thanks are expressed to Dr. Peter Byrne and Michael Beaty of UBC for providing the Liquefaction Triggering model used in the FLAC analyses.

References

Balakrishnan, A, and Kutter, B.L. (1999). Settlement, sliding and liquefaction remediation of layered soil. Journal of Geotechnical Engineering, ASCE, Vol. 125, No. 11, pp.968-978.

Beaty, M.H. and Byrne, P.M. (1999). Predicting liquefaction displacements with application to field experience. Proceedings of the Eighth Canadian Conference on Earthquake Engineering, June 13-16, 1999, Vancouver, B.C. pp. 335-340.

Byrne, P.M. and Janzen, W. (1985). *LATPILE – Deflections of laterally loaded piles.- Computer program and documentation.* Department of Civil Engineering, University of British Columbia, Vancouver, B.C.

Byrne, P.M. and Beaty, M.H. (1999). Assessment of residual strength for embankments. Proceedings of the Second International Conference on Earthquake Geotechnical Engineering, June 21-25, 1999, Lisboa, Portugal. pp. 1069-1075.

Castro, G. (1987). On the behavior of soils during earthquakes - Liquefaction. *Soil Dynamics and Liquefaction.* No. 42, pp.169-204. Edited by A.S.Cakmak, Published by Elsevier.

Crippen & Associates (1974). Pitt River Bridge – Upstream structure pile load test. Report presented to the B.C. Dept. of Highways by G.E.Crippen & Associates Ltd., North Vancouver, B.C, March 1974. – Private communication.

Hungr, O. (1988). *CLARA, Slope stability analysis in two or three dimensions for IBM or compatible microcomputers. V. 2.31.* O. Hungr geotechnical research Inc., West Vancouver, B.C..

Idriss, I.M. and Sun, J.I. (1992). *SHAKE91, A computer program for conducting equivalent linear seismic response analyses of horizontally layered soil deposits. Program modified based on the original SHAKE program published in 1972 by Schnabel, Lysmer and Seed.* University of California, Davis.

Interactive software designs (1996). *Slope stability program XSTABL, V. 5.2.* Interactive software designs, Inc., Moscow, Idaho.

ITASCA (1998). *FLAC – Fast lagrangian analysis of continua, Version 3.40.* ITASCA Consulting Group Inc., Thrasher Square East, 708 South Third Street, Suite 310, Minneapolis, Minnesota.

Kokusho, T. (1999). Water film in liquefied sand and its effect on lateral spread. Journal of Geotechnical Engineering, ASCE, Vol. 125, No. 10, pp.817-826.

MoTH (1998). Seismic safety retrofit and rehabilitation - Appendix C., Ministry of Transportation and Highways, B.C. – Private communication.

MoTH (1999). Pitt River seismic reflection survey - Ministry of Transportation and Highways, B.C. – Private communication.

Newmark, N.M. (1965). Effects of earthquakes on dams and embankments. 5th Rankine lecture, Geotechnique, Vol. 15, No. 2, pp. 139-160.

Seed, R.B. and Harder, L.F. (1990). SPT- Based analysis of cyclic pore pressure generation and undrained residual strength. Proceedings of the H. Bolton Seed Memorial Symposium, May 1990, BiTech Publishers, Ltd., pp. 351-376.

Seed, H.B. and Idriss, I.M. (1970). Soil moduli and damping factors for dynamic response analysis. Earthquake Engineering Research Centre Report, No. EERC 70-10, University of California, Berkley.

Seed, H.B. and Idriss, I.M. (1982). Ground motions and soil liquefaction during earthquakes. Earthquake Engineering Research Institute Monograph.

Sun, J.I., Golesorkhi, R. and Seed, H.B. (1988). Dynamic moduli and damping ratios for cohesive soils. Earthquake Engineering Research Centre Report, No. EERC 88/15, University of California, Berkeley.

Tokimatsu, K and Seed, H.B. (1987). Evaluation of settlements in sands due to earthquake shaking. Journal of Geotechnical Engineering, ASCE, Vol. 113, No. 8, pp.861-878.

Vucetic, M. and Dobry, R. (1991). Effect of soil plasticity on cyclic response. Journal of Geotechnical Engineering, ASCE, Vol. 117, No. 1, pp.89-107.

Yoshimi, Y., Tokimatsu, K., Kaneko, O. and Makihara, K. (1984). Undrained cyclic shear strength of a dense Niigata sand. Soils and Foundations, JSSMFE, Vol. 24, No. 4, pp.131-145.

Youd, T.L. and Idriss, I.M. (1997). *Proceeding of the NCEER workshop on evaluation of liquefaction resistance of soils.* Technical report NCEER-97-0022, December 31, 1997.